A novel non-registration based segmentation approach of 4D dynamic upper airway MR images : minimally interactive fuzzy connectedness

Yubing Tong[1], Jayaram K.Udupa[1], Dewey Odhner[1], Sanghun Sin[2], Mark E. Wagshul[3], Raanan Arens [2]

[1]Medical Image Processing Group, Department of Radiology, University of Pennsylvania, Philadelphia, PA

[2]Division of Respiratory and Sleep Medicine, The Children's Hospital at Montefiore, Albert Einstein College of Medicine, Bronx, NY

[3] Department of Radiology, Albert Einstein College of Medicine, Bronx, New York, NY

ABSTRACT

There are several disease conditions that lead to upper airway restrictive disorders. In the study of these conditions, it is important to take into account the dynamic nature of the upper airway. Currently, dynamic MRI is the modality of choice for studying these diseases. Unfortunately, the contrast resolution obtainable in the images poses many challenges for an effective segmentation of the upper airway structures. No viable methods have been developed to date to solve this problem. In this paper, we demonstrate the adaptation of the iterative relative fuzzy connectedness (IRFC) algorithm for this application as a potential practical tool. After preprocessing to correct for background image non-uniformities and the non-standardness of MRI intensities, seeds are specified for the airway and its crucial background tissue components in only the 3D image corresponding to the first time instance of the 4D volume. Subsequently the process runs without human interaction and completes segmenting the whole 4D volume in 10 sec. Our evaluations indicate that the segmentations are of very good quality achieving true positive and false positive volume fractions and boundary distance with respect to reference manual segmentations of about 93%, 0.1%, and 0.5 mm, respectively.

Keywords: 4D MR imaging, upper airway, segmentation, fuzzy connectedness.

1. INTRODUCTION

There are several disease conditions such as Polycystic Ovary Syndrome (PCOS) and Obstructive Sleep Apnea Syndrome (OSAS) that are associated with upper airway restrictive disorders. PCOS is one of the most common disorders associated with overweight and obesity and it affects 5-10% of adolescent girls and women of reproductive age. OSAS is common in obese children with risk being 4.5 fold compared to normal subjects. PCOS has recently been shown to be associated with OSAS that may further lead to significant cardiovascular and metabolic derangements in these subjects [1]. In the study of these conditions and their treatment methods, it is important to take into account the dynamic nature of the upper airway. As such dynamic imaging protocols have been investigated including MRI, CT, and Optical CT. While OCT offers high spatial and temporal resolution, it is somewhat intrusive, has poor depth of penetration, and has shadowing effects. CT affords good spatial and reasonable temporal resolution but has poor contrast resolution for soft tissue structures and has radiation concerns especially in the dynamic mode and in imaging children. Currently, therefore, dynamic MRI seems to be the modality of choice in studying these diseases [2].

Any effort (including modeling following computational fluid dynamics) to study quantitatively the upper airway and surrounding structures requires their segmentation as the fundamental step. Because of the sparse, tubular nature of the upper airway and surrounding hard and soft structures, the inadequate contrast resolution obtainable in the images leaves many challenges for an effective segmentation of the dynamic airway in 4D MR images. Due to the 4D nature of the images, manual or interactive segmentation becomes unacceptable in studying patient populations because of the requirement of immense human labor and time. Any practical method should be either fully automatic or call for minimal user interaction in segmenting each 4D MRI data set. No viable methods have been reported for the upper airway structures.

4D image segmentation strategies for breast, lungs, heart, great vessels, and brain have been reported in the literature [3-9]. Most of them employ a segmentation propagation approach wherein the image is segmented at one time point of the

Medical Imaging 2014: Biomedical Applications in Molecular, Structural, and Functional Imaging, edited by Robert C. Molthen, John B. Weaver, Proc. of SPIE Vol. 9038, 90380Z

4D volume first by using different techniques including manual segmentation, which is then propagated via image registration principles to images at other time points. 4D probabilistic atlases have also been attempted for the segmentation of cardiac structures. In this paper, we exploit the basic premise behind segmentation propagation of carrying over image and structure information from one time point to the next. We utilize the efficiency and competitive optimization capabilities of the fuzzy connectedness framework [10-12] to devise a practical solution to the upper airway 4D segmentation problem without requiring registration. We demonstrate the adaptation of the iterative relative fuzzy connectedness (IRFC) algorithm [12] for this application as a potential practical tool. IRFC is a top-of-the-line algorithm in the FC family [10, 11] which operates with the basic principles of FC but by iteratively reinforcing the segmentation evidence in a conservative manner. Like other FC members, it requires seeds to be specified in the object as well as in the background components. In our approach, the seeds are specified interactively on the images corresponding to only one time point and the rest of the 4D segmentation process proceeds without requiring human interaction.

2. MATERIALS & METHODS

Image data

The 4D dynamic MR images utilized in this paper were produced by the retrospective gating method described in [2]. In this process, image data acquisition was triggered only if the input respiratory signal was within pre-defined temporal and spatial tolerances. Abnormal volumes because of swallowing or coughing are recognized and discarded by the method. Images were collected on a 3T Philips Achieva scanner. A 3D, T1-weighted, inversion-prepared gradient echo sequence, acquired in the sagittal plane and reconstructed in the axial and coronal planes, was used for the study. Thirty six 1.1-mm thick sagittal slices were acquired with 30% oversampling in the slice encode direction. The slices were 240 x 240 with a pixel size of 1 mm x 1mm. 4D image data from 10 female subjects (PCOS and OSA) with 10 time points over the respiratory cycle were used in our experiments. Subjects were between 14 and 18 years of age, and MRI acquisition was in the wake condition without patient sedation.

Because of the non-standardness (lack of consistent tissue-specific numeric meaning for the intensity values) of the MR images, all 100 3D images were standardized [13]. Prior to standardization, intensity non-uniformities arising from magnetic field inhomogeneity were corrected [14].

Adaptation of the Iterative Relative Fuzzy Connectedness method

IRFC is a top-of-the-line algorithm in the FC family [10, 11]. The FC framework is graph-based. Let $I = (C, f)$ denote a 3D image where C is a rectangular array of voxels and f is the MR image intensity function. A graph (C, α) is associated with image $I = (C, f)$ where α is an adjacency relation on C such as 6-, 18-, or 26-adjacency. Each pair (c, d) of adjacent voxels in α is assigned an *affinity* value $\kappa(c, d)$ which expresses the strength of the bond between c and d in belonging to the same object. To each path π in the graph (or equivalently in I) in the set of all possible paths $\Pi_{a,b}$ between any two voxels a and b of C, a *strength of connectedness* $K(\pi)$ is determined, which is the minimum of the affinities between successive voxels along the path. The connectivity measure $K^*(a, b)$ between a and b is then defined to be $K^*(a, b) = \max \{K(\pi): \pi \in \Pi_{a,b}\}$. The notion of connectivity measure can be generalized to the case of "between a set A and voxel b" by a slight modification: $K^*(A, b) = \max \{K(\pi): \pi \in \Pi_{a,b} \,\&\, a \in A\}$. By using a fast algorithm to compute $K^*(A, b)$, the machinery of FC allows a variety of approaches to define and compute "objects" in images by specifying appropriate affinity functions and seed sets by means of how voxels hang together. All FC methods guarantee robustness to seed sets [11]. That is, if the seed set is changed to any set of voxels within a given segmentation produced by a given seed set, the same segmentation is guaranteed. This theoretical property plays an important role in the effectiveness of FC algorithms, particularly in the 4D adaptation described in this paper where seeds are propagated along the time axis.

A fuzzy connected object is defined with a threshold on the strength of connectedness for the basic FC method called Absolute FC. Relative fuzzy connectedness overcomes the need for a threshold and leads to more effective segmentations. The central idea is that an object gets defined in an image because of the presence of other co-objects [10]. Each object is initialized by a set of seed voxels. An image voxel c is considered to belong to that object with respect to whose reference seed voxels c has the highest strength of connectedness. IRFC [12] uses an iterative strategy for fuzzy connectedness calculation wherein the strongest relative connected core parts are first defined and iteratively relaxed to conservatively capture the more fuzzy parts subsequently. In IRFC, two seed sets A_O and A_B are indicated for an object O and its background B, respectively. Then the object indicated by A_O is separated from the background indicated by A_B by an iterative competition in connectivity measure between A_O and every voxel $c \in C$ and A_B and c. In

the adapted IRFC method, A_O and A_B are specified with human interaction in the 3D image corresponding to the first time instance of the 10-time point 4D image. Affinities $\kappa_O(c, d)$ and $\kappa_B(c, d)$ for O and B are designed separately. Subsequently they are combined into a single affinity κ by taking a fuzzy union of κ_O and κ_B. The same affinity is then propagated along the time axis. Each of κ_O and κ_B has two components. The description below is for κ_O. The same applies to κ_B.

$$\kappa_O(c, d) = w\psi_O(c, d) + (1\text{-}w)\varphi_O(c, d). \qquad (1)$$

Here, $\psi_O(c, d)$ represents a *homogeneity component* of affinity, meaning, the more similar image intensities $f(c)$ and $f(d)$ are at c and d, the greater is this component of affinity between c and d. $\varphi_O(c, d)$, the *object feature component*, on the other hand, describes the "degree of nearness" of the intensities at c and d to an intensity expected for the object O under consideration. For both ψ_O and φ_O, we use a Gaussian function with parameters $(m_{\psi O}, \sigma_{\psi O})$ and $(m_{\varphi O}, \sigma_{\varphi O})$ as follows.

$$\psi_O(c, d) = e^{-(f(c) - f(d))^2 / 2\sigma^2_{\psi_O}}. \qquad (2)$$

$$\varphi_O(c, d) = e^{-(\max\{f(c), f(d)\} - m_{\varphi_O})^2 / 2\sigma^2_{\varphi_O}}. \qquad (3)$$

The mean and standard deviation parameters are estimated from a few sample object- and background-tissue regions and then fixed. (This is why MRI non-uniformity correction and, more importantly, standardization become crucial.) For the airway object, a half-Gaussian form for (3) (that is, right portion of the bell curve only) is chosen centered at $m_{\varphi O}$, the idea being that if $f(c)$ and $f(d)$ are both lower than $m_{\varphi O}$ then this component of affinity should be maximum. The background tissue regions considered constitute essentially the tissue regions surrounding the airway: air outside the body region, hard palate, soft palate, tongue, and other soft structures around the airway. We set $w = 0.5$ and $\sigma_{\psi O} = \sigma_{\psi B}$. Once the affinity functions are specified, the IRFC process proceeds as follows.

To start off, in the 3D image corresponding to the first time point, we specify seed sets A_O and A_B in the different tissue components mentioned above. The IRFC algorithm is then run which results in a segmented binary volume. The algorithm then proceeds to the next time point by propagating seed sets from pervious to the next time point, and in this manner the entire respiratory cycle is covered. Since the background tissue regions move very little with respiration, we reuse the seed set A_B from the previous time point for the next time point. A_O in the next time point is determined by applying a morphological erosion operation to the binary segmented volume in the previous time point. All affinity functions remain the same throughout all time points. Once seeds (objects and background) are put in the right place as well as affinity parameters are set with the right values, IRFC performs precise segmentation.

3. EXPERIMENTS & EVALUATION

Among 10 subjects with PCOS whose dynamic data sets are utilized in our experiments, 4 subjects also had OSA. Only the sagittal data were used.

The IRFC algorithm has been integrated into the CAVASS software system [15] with a friendly and flexible user interface for interactive selection of seeds and training and setting up of affinity functions. Seeds (foreground and background) can be placed on any 2D slices. Once seeds and affinity functions are set, the computation of the 3D fuzzy connectedness map as a segmentation result is completed within seconds. In our experiments, foreground and background seeds were placed on 3 slices - one slice roughly centrally situated in the upper airway and the other two slices through the center of the left and right halves. Owing to the robustness of FC results with respect to seeds, just one or two foreground seeds are usually adequate. Background seeds are set in every organ around the target organ (whole pharynx). Since the background seeds are propagated to other time points unchanged, they must be set carefully so that they do not enter the airway structure in subsequent time points. This is easily checked quickly by examining the slices for subsequent time points.

In Figure 1, we display a slice at a fixed position and its 10 time points in the respiratory cycle from one of the test subjects along with the corresponding segmentations overlaid on the slices. Figure 2 demonstrates surface renditions of the airway structure segmented from this data set at ten time points. The segmentation results seemed visually acceptable in all 10 cases in our inspection of the slices as well as 3D renditions and animations of motion.

Direct evaluation of the segmentations as compared to manual delineations is shown in Figure 3 and Table 1. Segmentation accuracy [16] is expressed in terms of True Positive Volume Fraction (TPVF), False Positive Volume Fraction (FPVF), and Hausdorff Distance (HD) between the true and IRFC-found 3D boundary surfaces in Table 1.

Once seed sets are specified in the 3D image corresponding to the first time point, the proposed IRFC method takes about 10 seconds to segment an entire 4D image on a 4-core Intel Xeon 3.6 GHz machine with 8 GB RAM and running the linux-jb18.3.7.20-1.16 operating system.

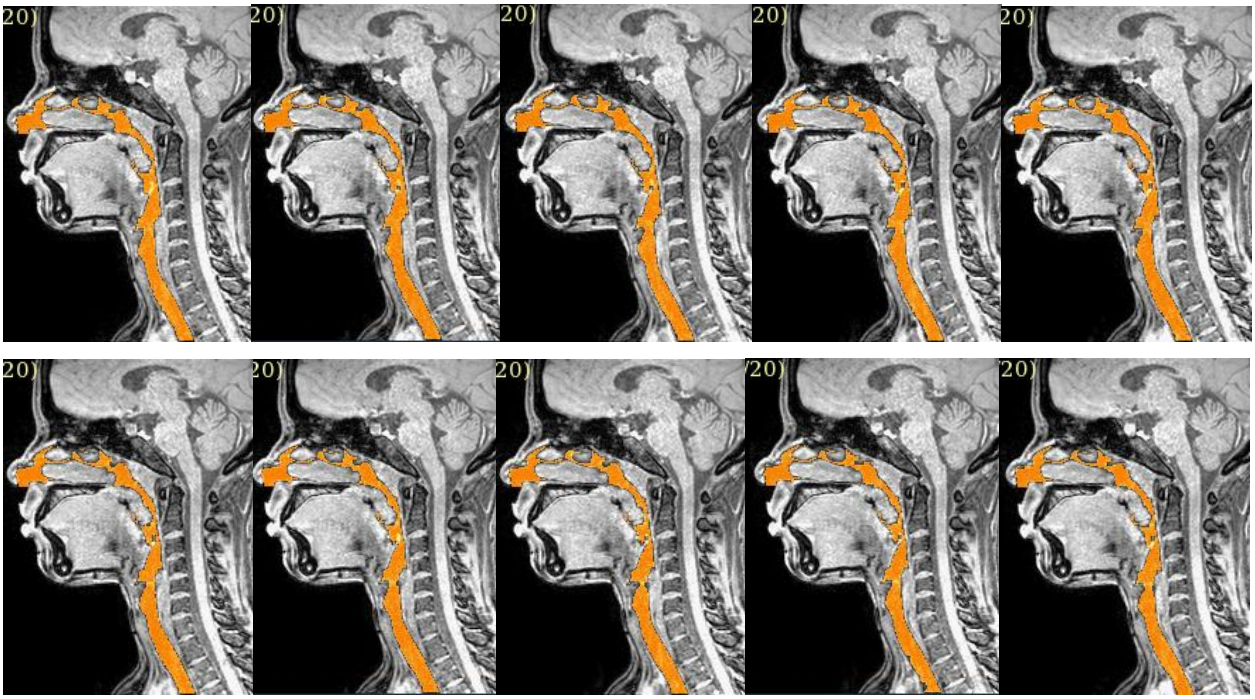

Figure 1. Segmentation results overlaid on slices over a full respiratory cycle for one fixed slice position for data from one subject.

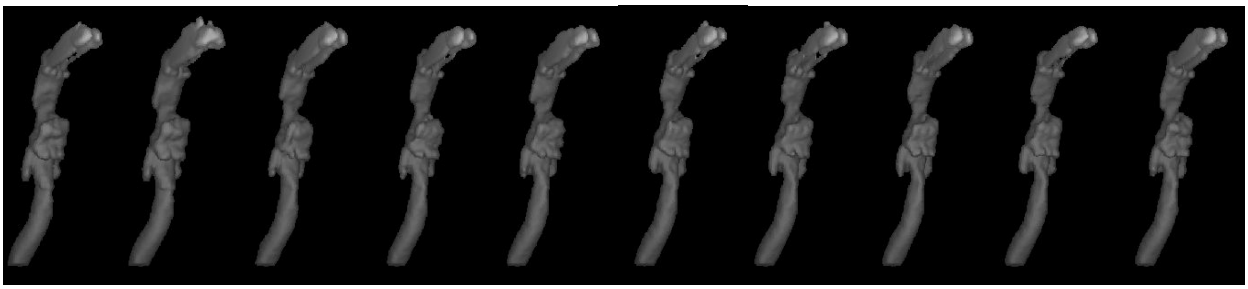

Figure 2. Surface renditions of the airway structure for all 10 time points for the subject data set shown in Figure 2.

Table 1. Quantitative evaluation of segmentations by comparing with manual segmentation. Mean values for each of the 10 time points T1-T10 over the 10 data sets are shown as well as the overall mean.

	T1	T2	T3	T4	T5	T6	T7	T8	T9	T10	Mean
TPVF (%)	93.38	93.18	93.61	94.18	93.25	92.19	93.40	93.30	92.46	91.90	93.08
FPVF (%)	0.10	0.11	0.12	0.12	0.11	0.12	0.13	0.15	0.14	0.14	0.12
HD (mm)	0.49	0.49	0.49	0.49	0.49	0.49	0.49	0.49	0.49	0.49	0.49

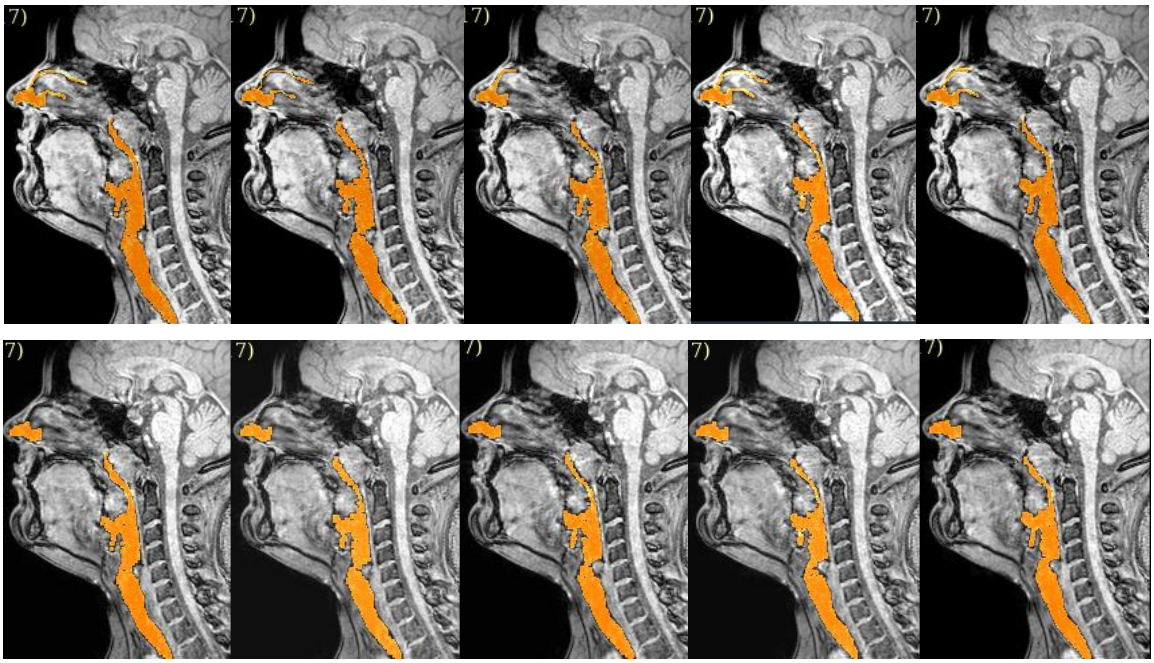

Figure 3. Comparison of IRFC result (bottom row) with manual segmentation (top row). Images from one subject corresponding to time points 2, 4, 6, 8, and 10 (left to right) are shown.

4. CONCLUSIONS

In the study of upper airway restrictive disorders, it is important to take into account the dynamic nature of the structures involved. Currently dynamic MRI is the only practical modality available for imaging these structures. Unfortunately, due to the poor contrast resolution obtainable in these dynamic images, no practical techniques for segmenting these structures have been demonstrated. With a combination of MR image processing and IRFC principles, combined with a careful identification of background tissue components that pose segmentation challenges with an understanding of the core strengths of IRFC, we have presented some evidence of the viability of a practical solution to this problem. After preprocessing to correct for background image non-uniformities and the non-standardness of intensities, seeds are specified for the airway and its crucial background tissue components. Seed specification is needed on several slices in only the 3D image corresponding to the first time instance of the 4D volume. Subsequently the process runs without human interaction and completes in 10 seconds for segmenting the whole 4D volume with a TPVF about 93%, a FPVF of about 0.1%, HD of about 0.5 mm as compared to manual segmentation.

This method seems to be the first demonstration of a practical approach for segmenting the upper airway structures in dynamic MR images. The method requires minimal user interaction and is very fast. In our preliminary comparison with a registration-based segmentation propagation approach, IRFC yielded better accuracy metrics (TPVF: 89% vs 93%, FPVF: 0.1% vs 0.3%, HD: both similar) and took far less computational time (3 min vs 10 sec).

A drawback of the current IRFC method is that background seed voxels must be specified carefully with knowledge of how the surrounding organs change with motion. Similarly care should be exercised in selecting seeds for the airway structures, especially in narrow regions. However, once the seeds are specified correctly, acceptable segmentations with high accuracy are produced rapidly.

ACKNOWLEDGEMENTS

The research reported here is supported by a DHHS grant HL105212.

REFERENCES

[1] Arens R., Sin S., Nandalike K., Rieder R., Khan UI., Freeman K., Wylie-Rosett J., Lipton ML., Wootton DM., McDough JM., Shifteh K., "Upper Airway Structure and Body Fat Composition in Obese Children with Obstructive Sleep apnea Syndrome," American Journal of Respiratory and Critical Care Medicine 183, 782-787(2011).
[2] Mark E. Wagshul, Sanghun Sin,Michael L. Lipton,Keivan Shifteh,and Raanan Arens. "Novel Retrospective, Respiratory Gating Method Enables 3D, High Resolution, Dynamic Imaging of the Upper Airway During Tidal Breathing 4D imaging," Magn Reson Med 70(6),1580-1590(2013).
[3] Badea CT, Johnston S, Johnson B, Lin M, Hedlund LW, Johnson GA.A. "Adual micro-CT system for small animal imaging," Proceeding of SPIE, 691342-10(2008).
[4] Darin Clark, Alexandra Badea, Yilin Liu, G.Allan Johunson, and Cristian T. Badea. "Registration-based segmentation of murine 4D cardiac micro-CT data using symmetric normalization," Phys Med Biol 57(19), 6125-6145(2012).
[5] Yang Y, Van Reeth E, Poh CL, Tan CH, Tham I. "A Spatio-Temporal Based Scheme for Efficient Registration-Based Segmentation of Thoracic 4D MRI," IEEE J Biomed Health Inform, www.ncbi.nlm.nih.gov/pubmed/24058039 (2013).
[6] Zhao F, Zhang H, Wahle A, Thomas MT, Stolpen AH, Scholz TD, Sonka M. "Congenital Aortic Disease: 4D Magnetic resonance segmentation and quantitative analysis," Med Image Anal 13(3),483-93(2009).
[7] Solomon J, Butman JA, Sood A. "Segmentation of brain tumors in 4D MR images using the hidden Markov model," Comput Methods Programs Biomed 84(2),76-85(2006).
[8] Jonhnson RK, Premraj S, Sonka M, Scholz TD. "Automated analysis of four-dimensional magnetic resonance images of the human aorta," Int J Cardiovasc Imaging 26(5), 571-8(2010).
[9] X. Zhuang, C. Yao, Y. L. Ma, D. Hawkes, G. Penney, and S. Ourselin, "Registration-based propagation for whole heart segmentation from compounded 3D echocardiography in Biomedical Imaging: From Nano to Macro," IEEE International Symposium on, 1093-1096(2010).
[10] Udupa, J.K., Saha, P.K., Lotufo, R.A.: "Relative fuzzy connectedness and object definition: Theory, algorithms, and applications in image segmentation," IEEE Transactions on Pattern Analysis and Machine Intelligence 24,1485-1500(2002).
[11] Udupa, J.K., Samarasekera, S.. "Fuzzy connectedness and object definition: Theory, algorithms, and applications in image segmentation," Graphical Models and Image Processing 58, 246-261(1996).
[12] Ciesielski, K.C., Udupa, J.K., Saha, P.K. and Zhuge, Y.: "Iterative relative fuzzy connectedness for multiple objects with multiple seeds," Computer Vision and Image Understanding 107(3),160-182, 2007.
[13] Nyúl LG, Udupa J. K. "On standardizing the MR image intensity scale," Magn Reson Med 42 (6),1072-81(1999).
[14] Ying Zhuge, Jayaram K. Udupa, Jiamin Liu, Punam K. Saha: "Image background inhomogeneity correction in MRI via intensity standardization," Comp. Med. Imag. and Graph Computerized Medical Imaging and Graphics 33(1), 7-16 (2009).
[15] Grevera, G., Udupa, J.K., Odhner, D., Zhuge, Y., Souza, A., Iwanaga, T. and Mishra, S.: "CAVASS: A computer assisted visualization and analysis software system," Journal of Digital Imaging 20(Supplement 1),101–118(2007).
[16] Udupa, J.K., LeBlanc, V.R., Zhuge, Y., Imielinska, C., Schmidt, H., Currie, L.M., Hirsch, B.E., Woodburn, J.: "A framework for evaluating image segmentation algorithms," Computerized Medical Imaging and Graphics 30(2), 75-87(2006).